

# Highly Efficient Silicon Photomultiplier for Positron Emission Tomography Application

Fei Sun, Ning Duan, and Guo-Qiang Lo

**Abstract**—A silicon photomultiplier (SiPM) was designed, fabricated and characterized. The SiPM was based on SACM (Separation of Absorption, Charge and Multiplication) structure, which was optimized for blue light detection in application of positron emission tomography (PET). The achieved SiPM array has a high geometric fill factor of 64% and a low breakdown voltage of about 22V, while the temperature dependence of breakdown voltage is only 17mV/°C. The gain and photon detection efficiency of the device achieved were also measured under illumination of light at 405nm and 460nm wavelengths. The gain of the device is in the order of  $10^6$ . The photon detection efficiency up to 60% has been observed under 1.8V overvoltage.

**Keywords**—Photon Detection Efficiency, Positron Emission Tomography, Silicon Photomultiplier.

## I. INTRODUCTION

FOR the past twenty-five years, detectors for Positron Emission Tomography (PET) have been based on photomultiplier tubes (PMT) as the photo detector of choice. The drawbacks of PMTs include fairly high cost, large size and high sensitivity to magnetic fields. In addition, most PET detector designs involve multiplexing a large number (e.g. 169) of scintillation crystals to a small number (e.g. 4) PMTs resulting in mispositioning errors, limited spatial resolution and dead time effects. To address these drawbacks, a number of groups have explored the possibility of using compact solid state photo detectors such as avalanche photodiodes (APDs) and more recently silicon photomultipliers (SiPMs). SiPMs have a much higher gain than APDs, with a similar gain to that of PMTs. In addition, they have much faster, sub-nanosecond, timing compared to APDs. Both APDs and SiPMs allow one-to-one coupling to the scintillator elements and are compatible with operation in a magnetic field [1]-[10]. SiPMs have therefore emerged as the photo detector of choice for compact PET detectors that are to be operated inside a magnetic field with minimal cross-interference of the PET and MRI operations.

In this paper, a SiPM array has been designed and fabricated, with a target for PET application. Some preliminary results of the device performances have been achieved.

This work was supported in part by the Biomedical Engineering Programme in the Singapore Agency for Science, Technology & Research (A\*STAR) under Project No. 1021480010

Fei Sun, Ning Duan and Guo-Qiang Lo are with Institute of Microelectronics, A\*STAR (Agency for Science, Technology and Research), Singapore. (phone: 65-6770-5495; fax: 65-6773-1914; e-mail: sunf@ime.a-star.edu.sg).

## II. DEVICE DESIGN

A SiPM array can be regarded as the parallel connection of many identical SiPM cells, each of which consists of an APD (avalanche photodiode) and a quenching resistor, as can be seen in Fig. 1 (a). Fig. 1 (b) shows the top view of a SiPM cell. The detection window of the APD is obviously smaller than the active region, because a certain amount of area was consumed by the contact via and metal wire. The active region has a square shape with rounded corners, which is necessary for suppression of the unwanted edge breakdown at sharp corners. We use poly-Si strips as quenching resistors. The resistance is expected to be in the order of  $10^5\Omega$  for effective quenching of the avalanche current.

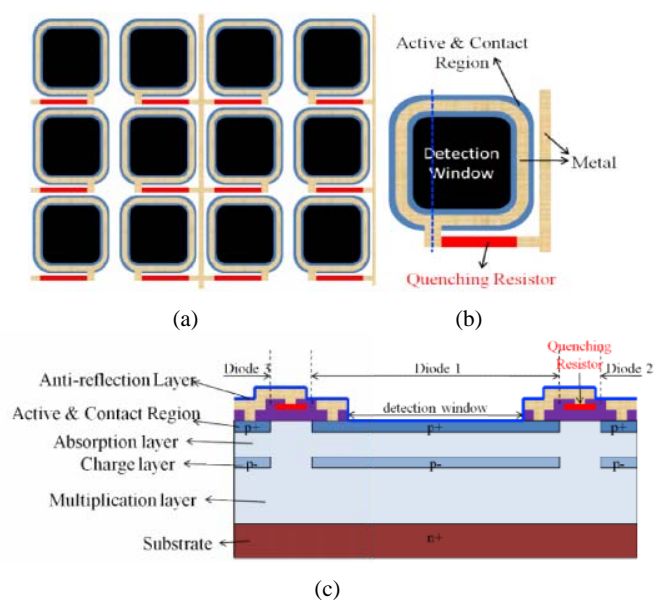


Fig. 1 (a) Schematic top-view of part of a SiPM array, (b) Top-view of a SiPM cell, (c) Cross-sectional view of a SiPM cell with SACM structure

Fig. 1 (c) shows the cross-sectional structure of the SiPM cell to be achieved. As can be seen, the Si APD was designed with a separate absorption, charge, and multiplication (SACM) structure, which includes an absorbing region and a multiplication region separated by a charge (to control electric field distribution between absorption region and multiplication region) region. When the APD is reversely biased, the electric field in the absorbing region will be much lower than in the multiplication region. The difference of the E-field value is determined by the doping level of the charge layer. Thus, the high electric field is confined in the buried multiplication

region. APD gain has a strong exponential dependence on the applied electric field strength. The E-field increases with increasing bias, causing the gain to increase rapidly until it reaches breakdown value of around 400kV/cm. Electrons, which are generated near the surface (absorption depth ~ 200nm) by blue light ( $\lambda= 420\text{nm}$ ), have a high probability to initiate impact ionization when they enter the high E-field region since they gained enough energy along the path. This buried junction enables single carrier injection instead of mixed injections, which leads to lower shot noise and higher speed. Electrons being the injection carriers are preferred than holes since they have higher ionization coefficient than holes in silicon.

The p+ layer in Fig. 1 (c) serves as active region of the APD, as well as the contact region for metal wire on top of APD. This region should be highly doped to guarantee the uniformity of electric field in absorption region and to achieve the good ohmic contact between metal and Si. However, high dopant concentration will result in recombination of photo-carriers generated in absorption region. Thus, the p+ layer is designed to be very thin (~100nm) in order to reduce the unexpected carrier losses, which is designed specifically for short wavelength. Absorption depth for 420nm wavelength in silicon is ~200nm, which means 63% of the light is absorbed in the first 200nm from the silicon surface. 40% of the total light is absorbed in the first 100nm distance, which is highly doped top contact layer.

### III. DEVICE FABRICATION

The devices designed were fabricated in clean rooms of IME lab. The SACM-based APD was achieved by Si epitaxial growth and ion implantation. The thickness of the multiplication layer in the SACM based APD was 600nm. The absorption layer was 200nm thick, which is sufficient for efficient absorption of blue light with the wavelength around 420nm. Thus the total thickness of Si epitaxial layer was only 800nm, which can help to reduce the breakdown voltage and the dark current of the device.

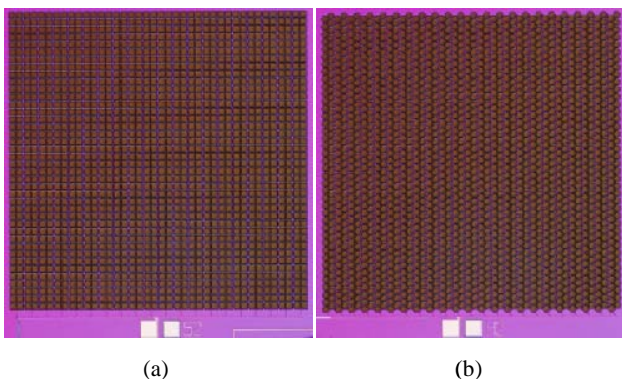


Fig. 2 Achieved  $2 \times 2 \text{mm}^2$  SiPM arrays based on (a) square cell and (b) hexagonal cell

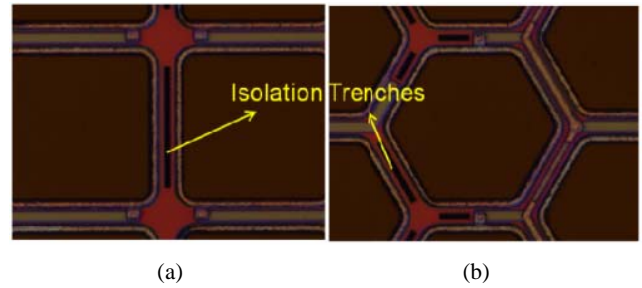


Fig. 3 Isolation trenches achieved in SiPM arrays between (a) square cells and (b) hexagonal cells

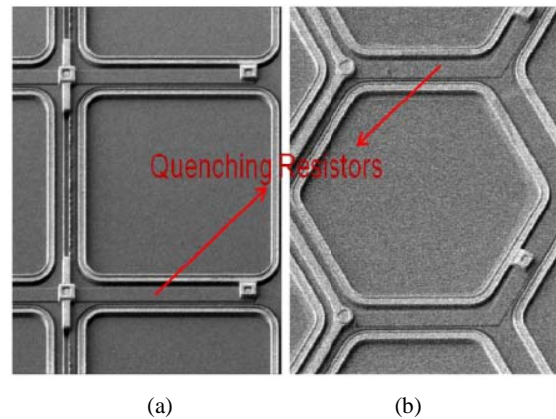


Fig. 4 SEM picture of poly-Si quenching resistors achieved in SiPM arrays based on (a) square cells and (b) hexagonal cells

Fig. 2 shows the top view of two achieved  $2 \times 2 \text{mm}^2$  SiPM arrays based on square cell and hexagonal cell, respectively. Fig. 3 shows the isolation trenches achieved between adjacent cells. As can be seen, the trenches were not introduced along all sides of the cells, because we didn't want to compromise the fill factor of the arrays. Since the isolation trenches will consume extra areas, the fill factor will be reduced if lower crosstalk is expected in future design. Fig. 4 shows the SEM pictures of SiPM cells where the poly-Si resistors can be clearly seen. Although the shapes of the resistors are different in square cells and hexagonal cells, their resistances are designed to be identical. According to our measurements, the resistance of a single poly-Si quenching resistor is about  $200 \text{k}\Omega$ , which is quite suitable for SiPM application.

### IV. CHARACTERIZATIONS

Fig. 5 shows the I-V and C-V curves of SiPM arrays we measured in IME. As can be seen, the breakdown voltage of the devices decreased to 22V. Further analysis shows that the linear relation between the device area and the dark current or capacitance of the device can still be observed. It should be mentioned that the I-V and C-V properties are not dependent on the cell shape. SiPM arrays based on square cells and hexagonal cells give identical measurement results.

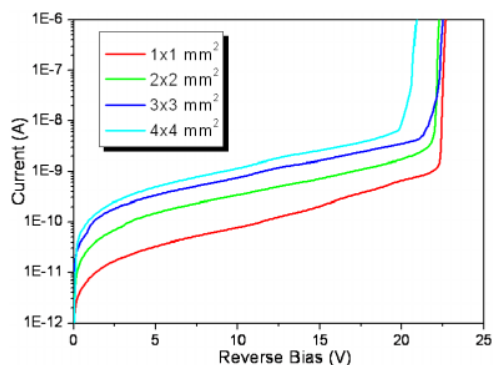


Fig. 5 I-V curves of SiPM arrays achieved

After the wafer-level characterization of I-V properties of the achieved devices, the wafer was diced into individual dies. The SiPM arrays were then connected to the PCB circuits by means of wire bonding. After that, the PCB was put into a thermal chamber to measure the temperature dependent I-V curves. One example of the measurement results is shown in Fig. 6. As can be clearly seen, with the increase of ambient temperature, the dark current increases while the breakdown voltage decreases. The thermal coefficient of the breakdown voltage is only 13~17mV/°C.

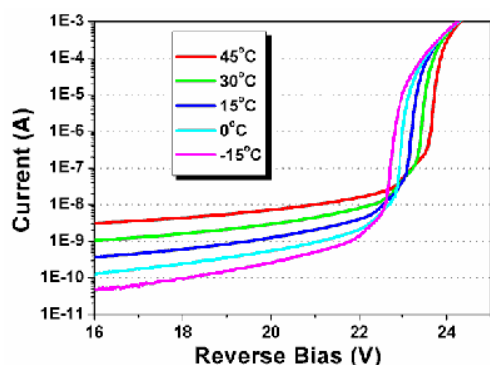


Fig. 6 Temperature dependence of dark current and breakdown voltage

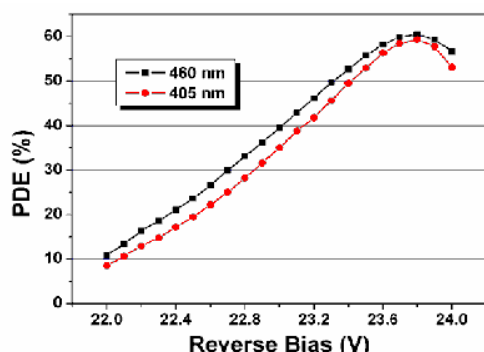


Fig. 7 Photon detection efficiency of a 1x1mm<sup>2</sup> SiPM array

The gain and photon detection efficiencies (PDE) of the devices were measured at -15°C by launching blue light (LED or laser) to the surface of the arrays. Two wavelengths, 405nm

and 460nm have been used for the measurements. One example of the PDE measurement results is shown in Fig. 7. As can be seen, the photon detection efficiency at either wavelength increases with the overvoltage, due to the increase of the gain. However, the noise of the device increases drastically with the overvoltage as well. When the noise goes so high that it is comparable to the light response, the PDE will become saturated and starts to decrease with further increase of the voltage applied. As shown in Fig. 7, a peak of PDE can be found when the overvoltage reaches to around 1.8V, where a PDE up to 60% can be achieved.

## V. CONCLUSION

We have successfully developed SiPM arrays with large size (up to 4x4mm<sup>2</sup>), high fill factor, large dynamic range, low dark current, low breakdown voltage, high temperature stability and high photon detection efficiency. This device will be very promising for PET application.

## ACKNOWLEDGMENT

The authors would like to thank Mr. Jose-Manuel Perez and Mr. Jesús Marín Muñoz in Centro de Investigaciones Energéticas, Medioambientales y Tecnológicas (CIEMAT, Madrid, Spain) for their kind assistances in device characterization and helpful discussions.

## REFERENCES

- [1] D. Renker, "A Geiger-mode avalanche photodiodes, history, properties and problems," *Nuclear Instruments and Methods in Physics Research A*, vol. 567, pp. 48-51, June 2006.
- [2] W. J. Kindt, N. H. Shahrjerdy, and H.W. van Zeijl, "A silicon avalanche photodiode for single optical photon counting in the Geiger mode," *Sensors and Actuators A*, vol. 60, pp. 98-102, 1997.
- [3] V. D. Kovaltchouk, G. J. Lolos, Z. Papandreou, and K. Wolbaum, "Comparison of a silicon photomultiplier to a traditional vacuum photomultiplier," *Nuclear Instruments and Methods in Physics Research A*, vol. 538, pp. 408-415, 2005.
- [4] J. A. Richardson, L. A. Grant, and R. K. Henderson, "Low dark count single-photon avalanche diode structure compatible with standard nanometer scale CMOS technology," *IEEE Photonics Technology Letters*, vol. 21, pp. 1020-1022, 2009.
- [5] P. Buzhan, B. Dolgoshein, L. Filatov, A. Ilyin, V. Kantzerov, V. Kaplin, A. Karakash, F. Kayumov, S. Klemin, E. Popova, and S. Smirnov, "Silicon photomultiplier and its possible applications," *Nuclear Instruments and Methods in Physics Research A*, vol. 504, pp. 48-52, 2003.
- [6] H. Moser, "Silicon detector systems in high energy physics," *Progress in Particle and Nuclear Physics*, vol. 63, pp. 186-237, 2009.
- [7] Y. Musienko, "Advances in multipixel Geiger-mode avalanche photodiodes (silicon photomultipliers)," *Nuclear Instruments and Methods in Physics Research A*, vol. 598, pp. 213-216, 2009.
- [8] N. Otte, "The silicon photomultiplier - A new device for high energy physics, astroparticle physics, industrial and medical applications," in *Proceedings of the International Symposium on Detector Development For Particle, Astroparticle and Synchrotron Radiation Experiments* Stanford, California, 2006, paper 0018.
- [9] D. J. Herbert, S. Moehrs, N. D'Ascenzo, N. Belcari, A. Del Guerra, F. Morsani, and V. Savelliev, "The silicon photomultiplier for application to high-resolution positron emission tomography," *Nuclear Instruments and Methods in Physics Research A*, vol. 573, pp. 84-87, 2007.
- [10] X. Li, C. Lockhart, T. K. Lewellen, and R. S. Miyaoka, "Study of PET detector performance with varying SiPM parameters and readout schemes," *IEEE Transactions on Nuclear Science*, vol. 58, pp. 590-596, 2011.